Springer

KSME

Journal of Mechanical Science and Technology 29 (8) (2015) 3395~3404
www.springerlink.com/content/1738-494x(Print)/1976-3824(Online)
DOI 10.1007/s12206-015-0737-2

A study on the behaviors of the D-ring with a curvature radius using the photoelastic experimental hybrid method †

Hyun-Seok Lim[1], Jai-Sug Hawong[1,*], Dong-Chul Shin[2], Alunda Ouma Bernard[1] and Kwang-Ho Lee[3]

[1]*School of Mechanical Engineering, Yeungnam University, Gyeongsan, Gyeongbuk, 712-749, Korea*
[2]*Department of Mechanical Engineering, Koje College, Geoje, Gyeongnam, 656-701, Korea*
[3]*Department of Automotive Engineering, Kyungpook Nat'l University, Sangju, Gyeongbuk, 742-711, Korea*

(Manuscript Received January 29, 2015; Revised June 2, 2015; Accepted June 9, 2015)

Abstract

Sealing is always a very important mechanical element when damage, breakage, leakage or even more serious disasters occur. Sealing has a range of cross-sections, such as O-rings, X-rings, Square-rings and D-rings, which is used in many ways. The cross section of a D-ring without curvature radius is simply combined with the half cross sections of an O-ring and Square-ring. The general D-ring has the same corner angle as the Square-ring's corner. Therefore, a stress concentration can easily cause damage. To reduce this stress concentration, a D-ring without curvature radius should be changed into a D-ring with a curvature radius on the square corner. Stress analysis of a D-ring with a curvature radius is needed. In this sturdy, the stress of a D-ring with a curvature radius under a uniform squeeze rate 20% and various internal pressures was analyzed by using a photoelastic experiment hybrid method. The results showed that the D-ring with a curvature radius has the advantages of both an O-ring and Square-ring, and the magnitudes of the contact stress in the D-ring with a curvature radius are almost constant along the contact line. This means that the packing ability of a D-ring with a curvature radius is excellent.

Keywords: Photoelastic experimental hybrid method; Uniform squeeze rate; Internal pressure; D-ring with a curvature radius; Contact stress; Packing ability; High pressure

1. Introduction

Sealing is used as packing element of the mechanical parts of high pressure equipment, such as the rocket propulsion parts, aircraft parts, hydraulic parts and other high-pressure sensitive parts. Damage, breakage or leakage in the sealing can result in serious disaster. Therefore, sealing is a very important element in the mechanical parts. The mechanics of the contact problems in the sealing is very important in the mechanics of sealing.

Hertz initially studied the contact problem [1]. He solved the size of the contact region and the magnitude of the contact pressure by assuming the distribution shape of the contact pressure on the material, for which theoretical analysis of the strength can be analyzed. Such contact problems include the point load applied to the elastic half plane, uniform pressure applied to the infinite half plane, rigid flat punch, and contact between one cylinder and another cylinder.

Sealing can be classified as O-ring, X-ring, Square-ring and D-ring. The usage of each ring is also various.

*Corresponding author. Tel.: +82 53 810 2445, Fax.: +82 53 810 4627
E-mail address: jshawong@ynu.ac.kr
† Recommended by Associate Editor Heung Soo Kim

Many researches exist on the behavior of O-ring [2-6], and a little exists on the stress distribution of square ring [7] or a stepped D-ring [8, 9]. It is suggested that sealing rings with square and half circular cross sectional configuration demonstrate better performance than O-ring or square when tested or used in the same groove designed for the O-ring [2].

The cross section of a general D-ring with is a combination of the half cross section of an O-ring and cross section of a square ring. Hence, a D-ring has the merits of an O-ring and square-ring. However, a general D-ring has square angle corner similar to a square-ring. Stress can concentrate easily at this corner (= inside square corner of D-ring, see Fig. 1), which can result in failure. If the D-ring has a rounded corner with a curvature radius, stress concentrations may be reduced. Therefore, a study on the stress distribution and deformation behavior of the D-ring with a curvature radius (Hereafter, "The suggested D-ring") is essential.

The photoelastic experimental hybrid method is a photoelastic experimental method in which the stress components (σ_X, σ_Y, τ_{XY}) can be separated by using isochromatic only without the use of isoclinics.

The stress distributions, change in cross section shape and contact length of an O-ring [5, 6], square-ring [7], stepped D-

ring [8, 9] and X-ring [10] have been studied by using this photoelastic experimental hybrid method.

In the present study, the stress distributions, forcing out, the behaviors of the contact lengths, and the change in the cross-section shape of the suggested D-ring under a uniform squeeze rate (20%) and internal pressure (7~20 MPa) were studied. The main goal of this study is a demonstration the superiority of the suggested D-ring under a uniform squeeze rate and internal pressure through the stress analysis by using the photoelastic experimental hybrid method. The additional purposes of this research are as follows:

(1) Contact stress analysis along the contact line of the suggested D-ring under various internal pressures.

(2) Observation of the variations of the contact length and isochromatic fringe patterns of the suggested D-ring according to the internal pressure.

(3) Internal stress analysis of the suggested D-ring exposed to various internal pressures.

2. Basic theory

2.1 Hertz contact theory

The stress components using Muskhelishvilli's complex function and the Airy stress function [11] are given by

$$\begin{aligned}\sigma_x &= \mathrm{Re}\left[2\phi(z)-\bar{z}\phi'(z)-\Psi(z)\right]\\ \sigma_y &= \mathrm{Re}\left[2\phi(z)+\bar{z}\phi'(z)+\Psi(z)\right]\\ \tau_{xy} &= \mathrm{Im}\left[\bar{z}\phi'(z)+\Psi(z)\right]\end{aligned} \tag{1}$$

where for convenience, $\phi(z)=\varphi'(z)$, $\Psi(z)=\psi'(z)$ and $z=x+iy$. The symbols 'Re' and 'Im' denote the real and imaginary parts of the complex variable, respectively.

Generally, a contact problem is a half-plane problem. If the body occupies the lower portion of the body, S- (z<0), an analytic complex function can be defined as follows [12]:

$$\Psi(z)=-\phi(z)-\overline{\phi(\bar{z})}-z\phi'(z). \tag{2}$$

By substituting Eq. (2) into Eq. (1), the stress equations can be obtained in terms of only one function, $\phi(z)$:

$$\begin{aligned}\sigma_x &= \mathrm{Re}\left[3\phi(z)+\overline{\phi(\bar{z})}+z\phi'(z)-\bar{z}\phi'(z)\right]\\ \sigma_y &= \mathrm{Re}\left[\phi(z)-\overline{\phi(\bar{z})}-z\phi'(z)+\bar{z}\phi'(z)\right]\\ \tau_{xy} &= \mathrm{Im}\left[-\phi(z)-\overline{\phi(\bar{z})}-z\phi'(z)+\bar{z}\phi'(z)\right].\end{aligned} \tag{3}$$

As shown in Eq. (3), the stress components can be determined readily by only determining the complex function $\phi(z)$. The stress function $\phi(z)$ is analytic, and can be expressed as a power series, as follows:

$$\phi(z)=\sum_{n=0}^{N}C_n z^{\frac{n}{2}}. \tag{4}$$

Finally, the stress components expressed by the power series can be obtained as follows:

$$\begin{aligned}\sigma_x(z) &= \sum_{n=1}^{N}\mathrm{Re}\left\{C_n\left[2F(n,z)-G(n,z)\right]+\bar{C}_nF(n,z)\right\}\\ \sigma_y(z) &= \sum_{n=1}^{N}\mathrm{Re}\left\{C_n\left[2F(n,z)+G(n,z)\right]-\bar{C}_nF(n,z)\right\}\\ \tau_{xy}(z) &= \sum_{n=1}^{N}\mathrm{Im}\left\{C_nG(n,z)-\bar{C}_nF(n,z)\right\}\end{aligned} \tag{5}$$

where $F(n,z)=\frac{n}{2}z^{\frac{n}{2}-1}$, and

$$G(n,z)=\frac{n}{2}\left[\left(\frac{n}{2}-1\right)\bar{z}-\frac{n}{2}z\right]z^{\frac{n}{2}-2}.$$

2.2 Photoelastic experimental hybrid method

The stress optic law for an isotropic material is given by [13]

$$\left(\frac{f_\sigma\cdot N_f}{t}\right)^2=(\sigma_x-\sigma_y)^2+(2\tau_{xy})^2. \tag{6}$$

By combining the actual experimental fringe data and the analytical assumed values for the stress components, an error can be generated that is never zero (see Eq. (8)). Therefore, a numerical method can be used to calculate and minimize these errors:

$$\left(\frac{f_\sigma\cdot N_f}{t}\right)^2-\left(\sigma_x-\sigma_y\right)^2-\left(2\tau_{xy}\right)^2=D(\varepsilon) \tag{7}$$

where f_σ is the stress fringe value, N_f is the isochromatic fringe order, t is the specimen thickness, and z represents the position coordinates ($z=x+iy$).

Eq. (8) is obtained by substituting Eq. (5) into Eq. (7). When the precise experimental data are substituted into Eq. (8), the equation becomes a function of only two coefficients, a_n and b_n of a complex variable; i.e., $C_n=a_n+ib_n$. The converging condition of $D(\varepsilon)\leq$ 10-5 was used in this study, and the errors almost converge to zero. By applying a numerical method [14] to Eq. (8) with the measured experimental data, a_n and b_n are determined, which satisfies the limit values of the errors:

$$D(\varepsilon)=\left(\frac{f_\sigma \cdot N_f}{t}\right)^2-\left\{\sum_{n=1}^{N}a_n \mathrm{Re}\left[2F(n,z)-2G(n,z)\right]+\sum_{n=1}^{N}b_n \mathrm{Im}\left[2F(n,z)+2G(n,z)\right]\right\}^2-\left\{\sum_{n=1}^{N}a_n \mathrm{Im}\left[2G(n,z)-2F(n,z)\right]+\sum_{n=1}^{N}b_n \mathrm{Re}\left[2F(n,z)+2G(n,z)\right]\right\}^2. \quad (8)$$

$C_n = a_n + ib_n$ were then substituted into Eq. (4) to determine the stress function $\phi(z)$ for a given experimental condition. Using Eq. (2), the stress function, $\Psi(z)$, is determined. When the determined stress functions are substituted into Eq. (1), the stress components for an arbitrary load can be determined. These processes are called the photoelastic experimental hybrid method.

3. Experiment and experimental method

The model material of the photoelastic experiment used in this study is a high temperature epoxy resin composed of Araldite B41 and harder HT-903(Hutsman Advanced Materials, Switzerland) at a weight ratio (Araldite : hardener) of 10:3.

Table 1 lists the mechanical properties of high temperature epoxy resin at 120˚C.

Figs. 1(a) and (b) show the geometrical dimensions, and the relationship between the local and global coordinates in the present study of the D-ring with a curvature radius of 0.7 mm at the inside square corner (Namely, "The suggested D-ring") used with the photoelastic experimental hybrid method. On the lower side, $x_l = X$ and $y_l = Y$. On the front region, $x_f = Y$ and $y_f = -X$. On the upper side, $x_u = -X$ and $y_u = -Y$. Based on the coordinate system, the contact length on each side was taken as the abscissa with the center of the contact length being the origin of the local coordinate system. A model of the photoelastic experiment, as shown in Fig. 1(a) was molded from a silicon mold.

Fig. 2 shows the experimental loading device for the D-ring at a uniform squeeze rate and internal pressure used in this study. The stresses of the model D-ring with a curvature radius of 0.7 mm under a uniform squeeze rate of 20% and various internal pressures were frozen at 120°C using the 3-dimensional photoelastic stress frozen method [5-10]. During the 3-D photoelastic experiment, the internal pressures were applied to the model D-ring using an internal pressure device.

Fig. 3 shows cylinder and cover with D-ring of loading device, and illustrates the path of applied oil.

A video microscope [10], at a magnification of 40x, was used to measure the contact lengths of the suggested D-ring.

The stress-frozen D-ring was sliced into the cross-section with 2 mm thickness. The contact lengths were measured. And then, the slices were polished until their thickness was about 0.4 mm.

Table 1. Mechanical properties of the high epoxy resin.

Mechanical property at 120˚C	Value
Elastic modulus (MPa)	15.6
Poisson's ratio	0.47
Hardening temperature (˚C)	120
Stress fringe value (N/m)	242.6

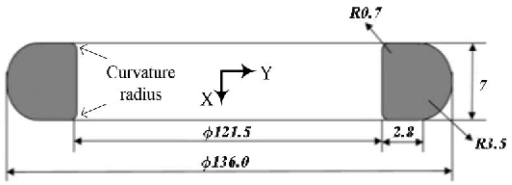

(a) Geometric dimensions of circular D-ring (Unit: mm)

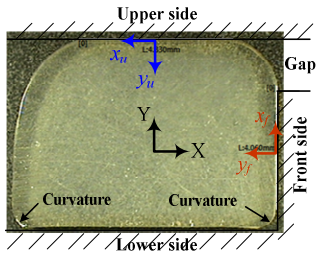

(b) Coordinate systems at a cross-section of the suggested D-ring

Fig. 1. Geometric dimensions, global (*X, Y*) and local coordinate system (*x, y*) of D-ring used in this study.

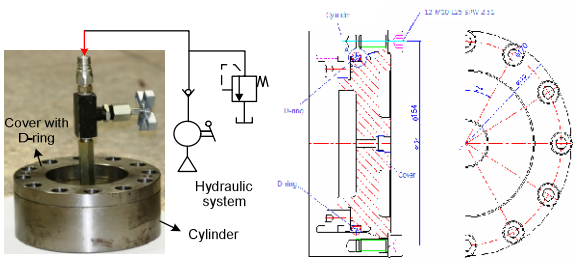

(a) Hydraulic loading device (b) Drawing of loading device

Fig. 2. Experimental loading device for the D-ring under a uniform squeeze rate of 20% and various internal pressures.

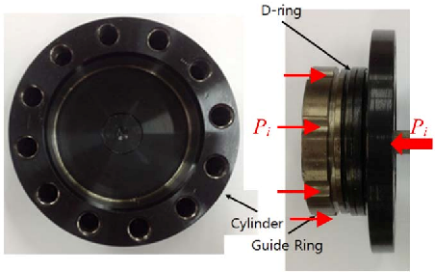

Fig. 3. Photographs of cylinder and cover with D-ring, and illustration for oil path ; The guide ring and D-ring is inserted into the cylinder.

The isochromatic fringe patterns using the transparent type photoelastic experimental device were recorded by a digital camera, and then transferred to a computer for analysis. The

measured experimental data was evaluated by using the stress optic law [13]. Hooke's and Jeeves' numerical method [14] was applied to the stress optic law with the experimental data. C_n was determined (n ~ 11 to 15).

The resulting C_n was substituted back into the stress optic law, and then the graphic isochromatic fringe patterns can be plotted. A comparison was made between the actual isochromatic fringes and the plotted isochromatic fringes. The stress components were finally determined when the graphic isochromatic fringes were identical to the actual isochromatic fringe patterns and the maximum shear stress contours (τ_{max}) were analogous to the actual isochromatic fringe patterns. If the patterns were not analogous, the process was repeated until the two patterns were identical and analogous.

4. Experimental results and discussion

Fig. 4 shows the actual isochromatic fringe patterns of the suggested D-ring under a uniform squeeze rate of 20% at various internal pressures. As shown in Fig. 4, the forcing out was occurred when internal pressure was 11 MPa. The internal pressure (11 MPa) is much higher than internal pressures of 3.92, 3.92 and 1.96 MPa of forcing out of the O-ring [5], Square-ring [7] and X-ring [10], respectively. In this study, "Forcing-out (or 'Gap extrusion' in Ref. [2])" is defined as a condition that the front side of a pressurized D-ring flows over the extension line from the laterally-constrained wall along the assembly gap of the loading device.

There is little difference between isochromatic fringe patterns of the suggested D-ring and those of the O-ring in the vicinity of points, in which the curvature begins.

A comparison of the isochromatic fringe patterns of the suggested D-ring with those of O-ring at the same internal pressure [5], isochromatic fringe patterns in the upper portion of the suggested D-ring are similar to those of the O-ring. In contrast, the isochromatics in the lower portion of the suggested D-ring are similar to those in which the isochromatic fringe pattern of the O-ring is spread along one side, but different to those of the square-ring [7].

Table 2. Contact length of D-ring with a curvature radius of 0.7 mm under various internal pressures and 20% squeeze rate.

Pressure (MPa)	Upper contact length [mm]	Front contact length [mm]
7	4.830	4.060
9	4.944	4.166
11	5.164	4.257
13	5.403	4.420
15	5.517	4.452
20	5.538	4.723

The square-ring, despite its stability, had a stress concentration at the lower corner, in which every designer wishes to avoid. The suggested D-ring has the advantages of both the O-ring in the upper part and a square-ring in the lower part. In other words, the distribution of isochromatic fringe patterns is more uniform (= uniform stress distribution) than that of the pure O-ring [5]. This is because the whole sealing material was interrupted from easily moving toward the front wall due to the square-shape of the lower part in the suggested D-ring (= the stability of the square-ring), and the half "O"-shape of the upper part protected the leakage of fluid through the upper contact path by the higher distributed contact stress (= the packing ability of O-ring). In addition, the stress concentration at the lower corner between the lower part and the front wall is relieved due to the existence of the curvature radius of 0.7 mm at the square corner in the suggested D-ring (= the reduction of the stress concentration). And the suggested D-ring is more excellent than the stepped D-ring [8, 9], on the stress concentration at the connecting point between the square shape and the half "O"-shape, because the connecting point in the suggested D-ring has a tangentially continuous connection, but not in the stepped D-ring.

Table 2 lists the contact length of the suggested D-ring under a range of internal pressures and 20% squeeze rates. As shown in Table 2, the contact length of the upper part and

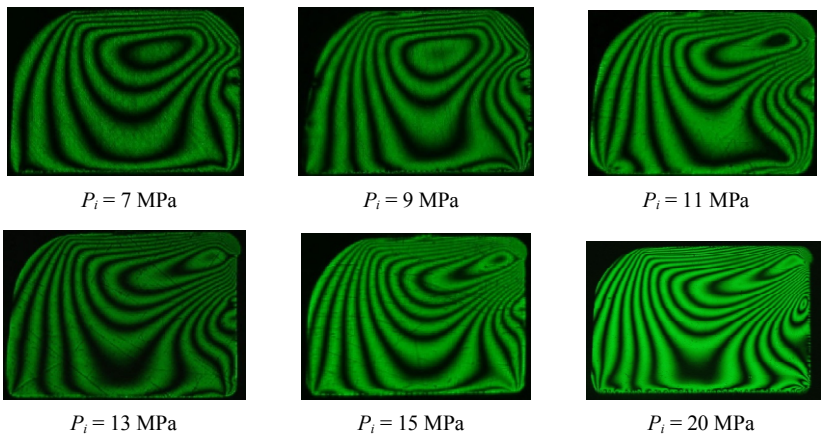

Fig. 4. Actual isochromatic fringe patterns of D-ring with a curvature radius of 0.7 mm under a squeeze rate of 20% at various internal pressures.

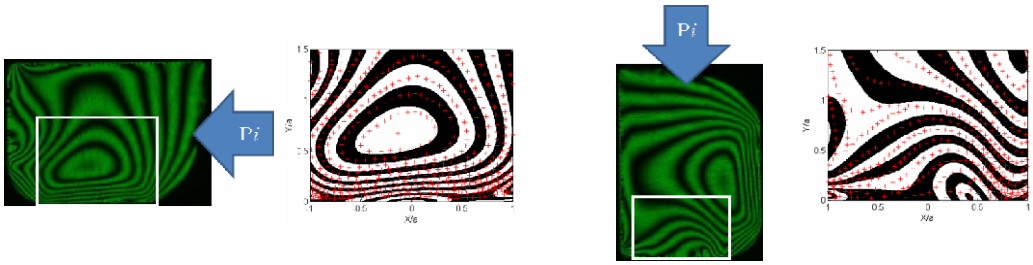

(a) Upper part (a = 2.472 mm) (b) Front part (a = 2.083 mm)

Fig. 5. Actual and graphic isochromatics of the D-ring with a curvature radius of 0.7 mm under a 20% squeeze rate (P_i = 9 MPa).

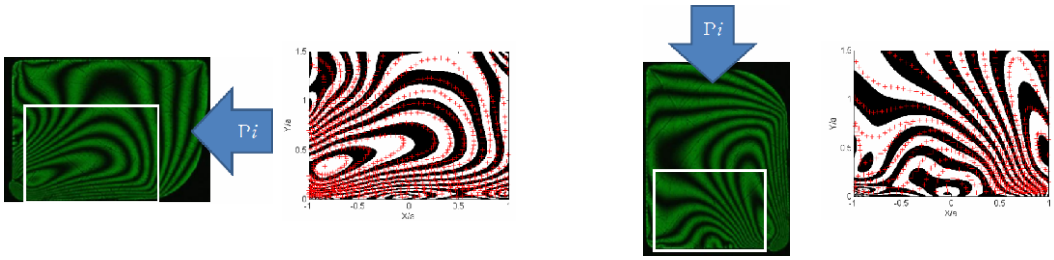

(a) Upper part (a = 2.702 mm) (b) Front part (a = 2.210 mm)

Fig. 6. Actual and graphic isochromatics of the D-ring with a curvature radius of 0.7 mm under a 20% squeeze rate (P_i = 13 MPa).

lower part of the suggested D-ring increases slightly with increasing internal pressure, the contact length of the upper part is longer than that of the front part of the suggested D-ring, and the increase in the contact length with the internal pressure of the upper part is greater than that of the lower part of the suggested D-ring. This means that the packing ability on the upper part is better than that on the front part of the suggested D-ring, and that the variation of contact length of the upper part is more sensitive to the internal pressures than that of the front part of the suggested D-ring.

From the variations of the isochromatic fringe patterns and the contact lengths, it was found that forcing out of the suggested D-ring occurs at a higher pressure than the pressures at which the forcing out of the O-ring, X-ring and square-ring occur. This means that the suggested D-ring is more effective than another sealing ring in the high pressure system.

Figs. 5(a) and (b) show the actual and the graphic isochromatic patterns in the upper part and the front part of the suggested D-ring at a squeeze rate of 20%, respectively, when the internal pressure (= P_i) is 9 MPa. Here, the isochromatics of the left and the right sides are the actual isochromatics and the graphic isochromatics, respectively. The graphic isochromatics were obtained by using the photoelastic experimental hybrid method. The data points were measured inside the rectangular (□) region on the actual isochromatic fringe patterns. The crosses (+) marked on the graphic isochromatic fringe patterns indicate the points at which the experimental data was obtained. The experimental data were measured along the center line of the white or the dark bands (which means each integer and integer plus 0.5 orders) of the actual isochromatics. These cross marks (+) must be located almost along the center line of the white and dark bands of the graphic isochromatics. These point data and the fringe orders at each point, together with the stress fringe value and thickness of the specimen, were used with the photoelastic experimental hybrid method to obtain the graphic isochromatic fringe patterns, stress components (σ_X, σ_Y, τ_{XY}), principal stresses, maximum shear stress ($\tau_{\max}$), and von Mises equivalent stresses.

As shown in Fig. 5, the graphic isochromatic fringe patterns are identical to the actual ones and all cross marks are located along the center line of the white or the black bands. Therefore, the photoelastic experimental hybrid method used in this study is valid for the stress analysis of the suggested D-ring.

Figs. 6 and 7 show the isochromatics in the upper part (Figs. 6(a) and 7(a)) and the front part (Figs. 6(b) and 7(b)) of the suggested D-ring. The graphic isochromatics were also obtained by using the photoelastic experimental hybrid method.

Figs. 5 and 6 show that the fringe orders of the isochromatics increased with increasing internal pressures, and the density of the isochromatic fringes around the assembly gap is quite high after forcing out, that is, the stress gradient becomes large. Therefore, it can be easily predicted that the maximum shear stress in the suggested D-ring occurs around the assembly gap.

The change of the isochromatic fringe orders in the lower part (Namely, upper portion of (a) and right portion of (b) in the Figs. 5-7) with increasing the internal pressure are small, while the increment variations of isochromatic fringe orders in the front and upper part are quite large compared those in the lower part. This situation means that the sealing effect of the suggested D-ring is more related to the magnitudes of the contact stress around the assembly gap between the front part

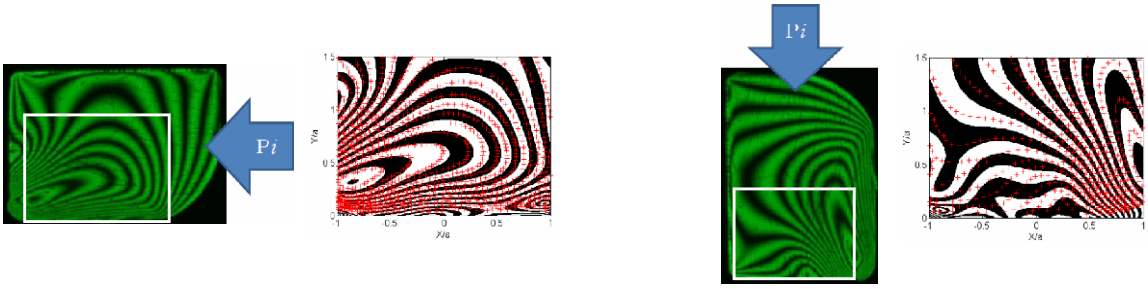

(a) Upper part (a = 2.759 mm) (b) Front part (a = 2.226 mm)

Fig. 7. Actual and graphic isochromatics of the D-ring with a curvature radius of 0.7 mm under a 20% squeeze rate (P_i =15 MPa).

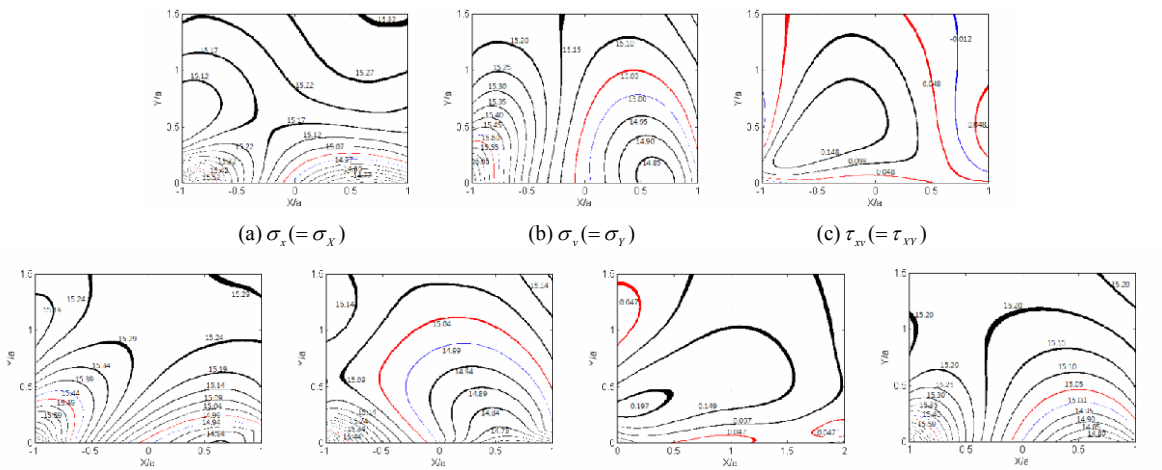

(a) $\sigma_x (= \sigma_X)$ (b) $\sigma_v (= \sigma_Y)$ (c) $\tau_{xy} (= \tau_{XY})$

(d) σ_1 (e) σ_2 (f) $\tau_{\max}$ (g) σ_{VM}

Fig. 8. Stress contours in the upper part of the D-ring with a curvature radius of 0.7 mm under 20% squeeze rate and an internal pressure of 15 MPa ($x_u = x = -X$, $y_u = y = -Y$).

and the upper parts of the suggested D-ring than the magnitudes of contact stresses of the lower part.

According to previous studies, the fracture is initiated at the assembly fillet part of the assembly gap portion in most sealing system. This is dependent on the maximum shear stress criterion that the fracture initiates at the point at which the maximum shear stress occurs. The maximum shear stress will be occurred at the point that the gradient of isochromatic fringe is steepest and the fringe order is also highest. Therefore, these results show that it is possible to estimate the point at which the fracture of the sealing material is initiated.

The detailed stress analyses of the suggested D-ring with the internal pressures from 7 to 20 MPa were performed. However, only a detailed analysis of the suggested D-ring at a uniform squeeze rate of 20% and an internal pressure of 15 MPa is reported in this paper for the sake of brevity.

Fig. 8 shows the internal stress contours, σ_X, σ_Y, τ_{XY}, and the maximum shear stress distribution, $\tau_{\max}$, and the principal stresses σ_1, σ_2, and the von Mises stress σ_{VM} in the upper part of the suggested D-ring at a uniform squeeze rate of 20% and an internal pressure of 15 MPa. From these results, the highest values of the contact stresses, σ_X, σ_Y and τ_{XY} are 16.15, 15.78 and 0.06 MPa, respectively. In addition, σ_1, σ_2, $\tau_{\max}$, and σ_{VM} are 16.15, 15.78, 0.19, and 15.97 MPa, respectively. The stress contours in the upper part show that the region close to the extrusion gap is highly stressed.

The stress contours shown in Fig. 9 represent the distributions of the interior stresses, and the maximum shear stress etc. in the front part of the suggested D-ring under a uniform squeeze rate of 20% and an internal pressure of 15 MPa. The highest values of contact stresses, σ_X, σ_Y and τ_{XY} are in these regions are 15.20, 15.16 and 0.06 MPa, respectively. In addition, σ_1, σ_2, $\tau_{\max}$ and σ_{VM} are 15.22, 15.11, 0.17 and 15.15 MPa, respectively. The stresses in the upper part were shifted slightly to the right compared to those of the pure Hertzian contact stress. The highest magnitudes of the σ_{VM} stresses are much higher than those of $\tau_{\max}$ in the upper and front parts. It is noted that the maximum stresses (σ_1) and the minimum stresses (σ_2) on the upper side were higher than those of the front side.

Fig. 10 shows the variations of the contact stress component (σ_X, σ_Y and τ_{XY}) along the contact length with internal pressure of the upper part in the suggested D-ring under various internal pressures and a uniform squeeze rate (20%). As shown in Fig. 10, σ_X and σ_Y increased with increasing

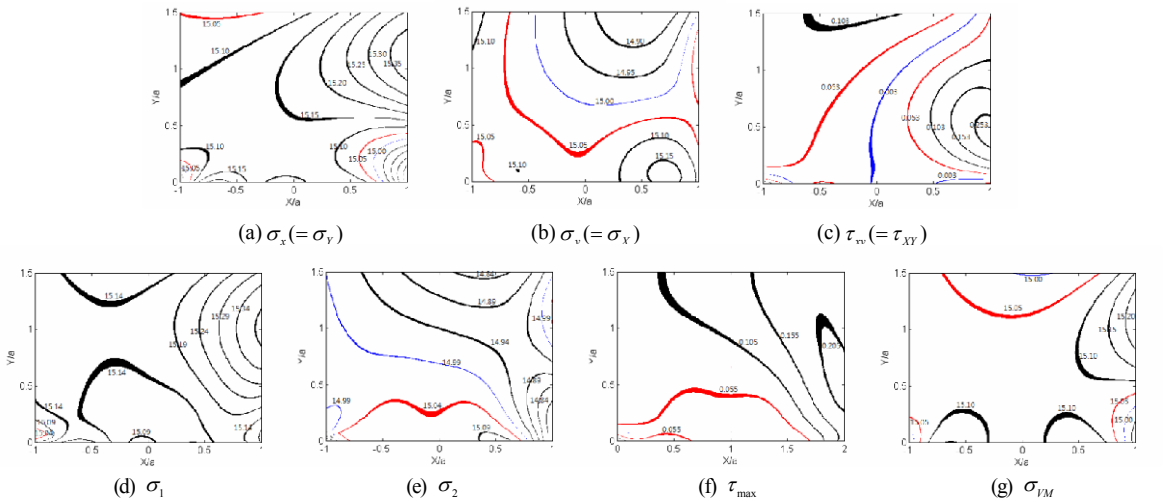

(a) $\sigma_x (= \sigma_Y)$ (b) $\sigma_v (= \sigma_Y)$ (c) $\tau_{xy} (= \tau_{XY})$

(d) σ_1 (e) σ_2 (f) $\tau_{\max}$ (g) σ_{VM}

Fig. 9. Stress contours in the front part of the D-ring with a curvature radius of 0.7 mm under a 20% squeeze rate and an internal pressure of 15 MPa ($x_f = x = Y$, $y_f = y = -X$).

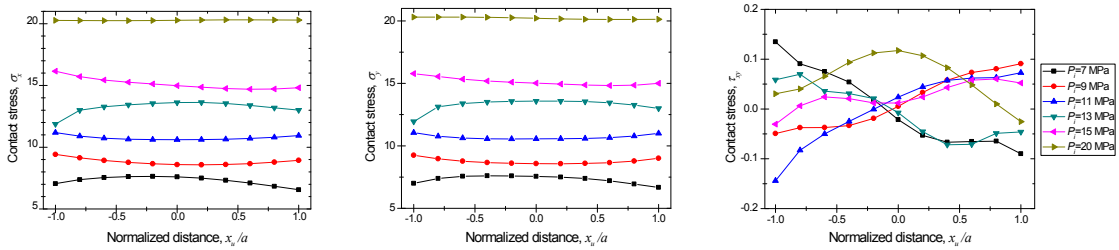

(a) σ_X (b) σ_Y (c) $\tau_{xy} (= \tau_{XY})$

Fig. 10. Variations of the contact stresses of the upper part in the D-ring with a curvature radius of 0.7 mm under various internal pressures and a uniform squeeze rate (20%).

internal pressure and they were almost constant along the contact length. This means that the suggested D-ring has very good packing ability. The distribution configuration of stress σ_X was similar to that of the stress σ_Y. The stresses around the assembly gap decreased slightly at internal pressure of 13 MPa just after forcing out, and then at internal pressure 15 MPa, similar behaviors as at the previous internal pressures were produced.

In the O-ring, the maximum contact stress occurs around the center and the magnitude of the contact stresses decreased with approaching the end points of contact, i.e., the distribution configuration of the contact stress in O-ring is "∩", while almost constant along the contact length in the suggested D-ring.

The τ_{XY} sign of the upper part in the suggested D-ring is changed at the center of contact. In addition, the magnitudes of τ_{XY} were considerably small compared to those of σ_X and σ_Y, which suggests that the isochromatic fringe patterns of the suggested D-ring under a uniform squeeze rate (20%) and various internal pressure are occurred from the difference between the σ_X magnitude and σ_Y magnitude, and that the magnitudes of the principal stresses σ_1 and σ_2 are similar to those of σ_X and σ_Y. These results are similar to those of O-ring [5].

Fig. 11 presents the distribution of contact stresses σ_1, σ_2, von Mises equivalent stress σ_{VM} and maximum shear stress $\tau_{\max}$ along the contact line of the upper part in the suggested D-ring under various internal pressures and a uniform squeeze rate of 20%. Fig. 11 shows that the magnitude of the principal stresses σ_1 and σ_2 are similar to those of σ_X and σ_Y, their magnitudes increase with increasing internal pressures and their magnitudes are relatively constant along the contact path. After forcing out, the maximum σ_1 and σ_2 occurs around the assembly gap (x_u/a = -1). The maximum shear stress occurs around the assembly gap. The behaviors of the von Mises equivalent stress are similar to those of the principal stresses

Fig. 12 shows the variations of the contact stresses with the internal pressures along the contact line of the front in the suggested D-ring under various internal pressures and a uniform squeeze rate (20%). The magnitudes of σ_X and σ_Y also increased with increasing internal pressures. Their magnitudes were relatively constant along the contact line. The distributions and magnitudes of the stress σ_X are similar to those of the stress σ_Y. The magnitudes of τ_{XY} of the front part in the suggested D-ring under various internal pressures

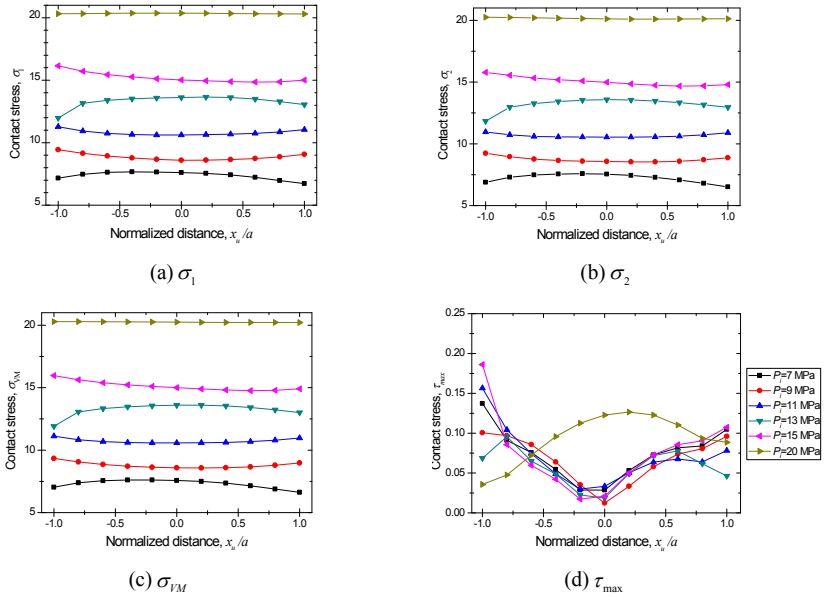

Fig. 11. Variations of the calculated contact stresses of the upper part in the D-ring with a curvature radius of 0.7 mm under the internal pressures and a uniform squeeze rate (20%).

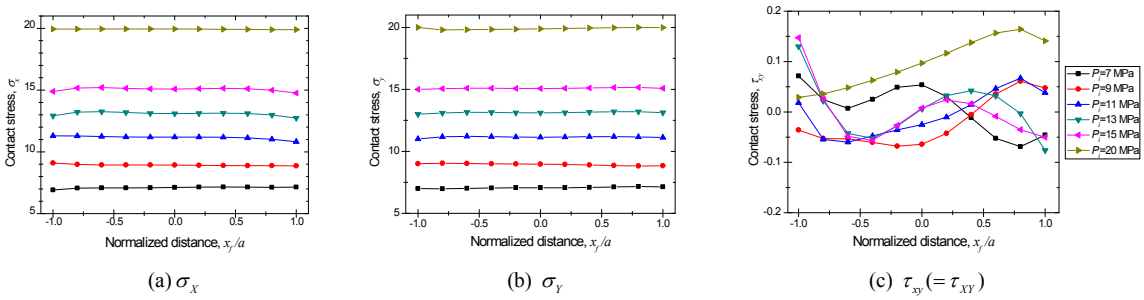

Fig. 12. Variations of the contact stresses of the front part in the D-ring with a curvature radius of 0.7 mm under various internal pressures and a uniform squeeze rate (20%).

and a uniform squeeze rate of 20% is very small compared to those of σ_X and σ_Y, as observed with the results from the upper part in the suggested D-ring.

The variations of τ_{XY} of the front part in the suggested D-ring were relatively large. These results were attributed to the characteristic isochromatic fringe pattern produced at the center part of the front part in the suggested D-ring. This shows that those characteristic isochromatic fringe patterns occurred due to the connecting portion between the square shape and the "O"-shape at the center part of the front part in the suggested D-ring.

Fig. 13 shows variations of the contact stresses along the contact line of the front part in the suggested D-ring under various internal pressures and a uniform squeeze rate of 20%. The distributions of the contact stress along the contact line of the front part are similar to those of the upper part in the suggested D-ring. But, the distributions and magnitudes of the maximum shear stress τ_{max} around the assembly gap of the front part in the suggested D-ring were significantly higher than of another part in the suggested D-ring after forcing out. These results are related to the situation that the fracture of most sealing materials occurs around the assembly gap, i.e., the maximum shear stress criterion is more effective than the maximum normal stress theory.

Figs. 10-13 show that the contact stress (σ_X, σ_Y, σ_1, σ_2 and σ_{VM}) distributions and stress (σ_X, σ_Y, σ_1, σ_2 and σ_{VM}) magnitudes of the front part in the suggested D-ring along the contact line are more uniform and smaller than those of the upper part, respectively, that the shear stress (τ_{XY} and τ_{max}) distributions of the upper part are more uniform than those of the front part in the suggested D-ring, and that the magnitudes of the shear stress (τ_{XY} and τ_{max}) of the upper part are similar to those of the front part in the suggested D-ring. The magnitude sequence (Order) of the contact stresses of the upper and the front part in the suggested D-ring is σ_1, σ_X, σ_{VM}, σ_Y, σ_2, τ_{max}, and τ_{XY}.

The contact stresses of the upper part are greater than those of the lower part in the suggested D-ring. In the sealing system, there are two paths through which the fluid can leak. One is the upper path on the upper part of the packing ring. Another is the lower path underneath the lower part of the packing ring plus the front path on the front part of the packing ring. The

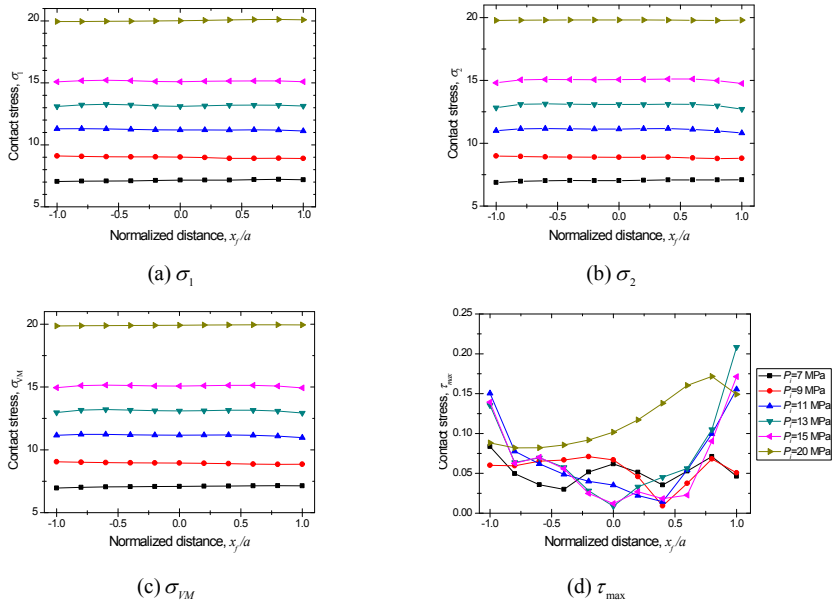

Fig. 13. Variation of the calculated contact stresses of the front part in the D-ring with a curvature radius of 0.7 mm under various internal pressures and a uniform squeeze rate (20%).

length of the latter is longer than that of the former. Therefore, the fluid can leak more easily along the upper leakage path than the lower leakage path.

The magnitudes of the contact stresses of the upper part in the suggested D-ring are greater than those of the lower part or the front part in the suggested D-ring.

Figs. 10-13 show that the upper part in the suggested D-ring has the benefits of O-ring in the upper part and square-ring in the lower part, and reduce stress concentration in the case of the stepped D-ring in the front part. In other words, the suggested D-ring maintains the stability of a square-ring and reduces the stress concentration of the stepped D-ring and relieves the stress concentration at the lower square corner because of the existence of the curvature radius. Therefore, these results confirmed that the suggested D-ring has advantages of both the O-ring and Square-ring, and the packing ability of the suggested D-ring is excellent.

5. Conclusion

The following conclusions were drawn based on the study of the suggested D-ring under a 20% uniform squeeze rate and various internal pressures using the photoelastic experimental hybrid method.

(1) The suggested D-ring has both advantages of the O-ring and square-ring, and relieves the stress concentration at the lower square corner because of the existence of the curvature radius. The packing ability of the suggested D-ring is also excellent.

(2) The increment of isochromatic fringe order of the upper part in the suggested D-ring is much greater than that of the lower part in the suggested D-ring. This means that the packing ability on the upper part in the suggested D-ring is more effective than underneath the lower part.

(3) The variation of the contact length of the upper part in the suggested D-ring under various internal pressures is more sensitive than that of the front part and the lower part. These results mean that the contact portion on the upper part in the suggested D-ring has a larger influence on the packing ability than the other portion.

(4) Magnitude sequence (Order) of the contact stresses of the upper part and the front part in the suggested D-ring is σ_1, σ_X, σ_{VM}, σ_Y, σ_2, $\tau_{\max}$, and τ_{XY}. The magnitudes of all contact stresses of the upper part in the suggested D-ring are greater than those of the front part. This means that the packing ability on the upper part in the suggested D-ring is better than that on the front part.

(5) Shear stress (τ_{XY} and $\tau_{\max}$) distributions of the upper part in the suggested D-ring are more uniform than those of the front part. The magnitudes of shear stress of the upper part in the suggested D-ring are similar to those of the front part.

(6) The distributions and magnitudes of the contact stress (σ_X, σ_Y, σ_1, σ_2 and σ_{VM}) of the upper part in the suggested D-ring along with the contact line are larger than those of the front part, and more uniform than those in the O-ring under the same loading conditions.

References

[1] H. Hertz, *Miscellaneous Papers*, translated by D.E. Jones and G. A. Shott, Macmillan, New York (1896).

[2] *Parker O-ring handbook ORD 5700,* Eriks Sealing Elements Technical Handbook for O-rings (2007).

[3] F. George, A. Strozzi and J. I. Rich, Stress fields in a com-

pressed unconstrained elastomeric O-ring seal and a comparison of computer predictions with experimental results, *Tribol. Int*., 20 (1987) 237-247.

[4] E. Dragoni and A. Strozzi, Theoretical analysis of an unpressurized elastomeric O-ring seal into a rectangular groove, Elsevier Sequioa, *Wear*, 130 (1989) 41-51.

[5] J. H. Nam, J. S. Hawong, S. L. Han and S. H. Park, Contact stress of O-ring under uniform squeeze rate by photoelastic experimental hybrid method, *J. of Mech. Sci. and Tech.*, 22 (12) (2008) 2337-2349.

[6] J. H. Nam, J. S. Hawong, Y. Liu and D. C. Shin, 3-Dimensional stress analysis of O-ring under uniform squeeze rate and internal pressure by photoelastic experimental hybrid method, *J. of Mech. Sci. and Tech.*, 25 (9) (2011) 2447-2455.

[7] A. B. Ouma, J. Nam, L. H. Seok and J. S. Hawong, A study on the contact stress of square ring under uniform squeeze rate and internal pressure by photoelastic experimental hybrid method, *J. of Mech. Sci. and Tech.*, 26 (8) (2012) 2617-2626.

[8] B. R. Mose, J. S. hawong, B. O. Alunda, L. H. Seok and J. Nam, Evaluating the stresses of a stepped unrounded D-ring under uniform squeeze rate and internal pressure by photoelastic experimental hybrid method, *J. of Mech. Sci. and Tech.*, 26 (8) (2012) 2603-2616.

[9] B. R. Mose, J. H. Nam, L. H. Seok and J.-S. hawong, Internal stress analysis of a stepped rounded D-ring under a uniform squeeze rate and internal pressure using a photoelastic experimental hybrid method, *J. of Mech. Sci. and Tech.*, 27 (8) (2013) 2413-2423.

[10] D.-C. Shin, J.-S. Hawong, S.-W. Lee, A. O. Bernard and H.-S. Lim, Contact behavior analysis of X-ring under internal pressure and uniform squeeze rate using photoelastic experimental hybrid method, *J. of Mech. Sci. and Tech.*, 28 (8) (2014) 4063-4073.

[11] N. I. Muskhelishvili, *Some basic problems of mathematical theory of elasticity*, 4th Edition, P. Noordhoff Ltd., Groningen Netherlands (1963).

[12] D. A. Hills, D. Nowell and A. Sackfield, *Mechanics of elastic contacts*, Butterworth-Heinemann, USA (1993).

[13] R. C. Sampson, A stress-optic law for photoelastic analysis of orthotropic composites, *Experimental Mechanics*, 10 (1970) 210-215.

[14] M. S. Bazaraa and C. M. Shetty, *Nonlinear programming theory and algorithms*, John Wiley & Sons Inc., USA (1979).

Jai-Sug Hawong received his B.S. degree in Mechanical Engineering from Yeungnam University in 1974. He received his M.S. degree from Yeungnam University in Korea in 1976, and Ph.D. degree from Kanto Gakuin University in Japan in 1990. He is currently a Professor at the School of Mechanical Engineering at Yeungnam University in Gyeongsan City, Korea. He served as President of the Korea Society of Mechanical Engineering. Prof. Hawong's research interests include static and dynamic fracture mechanics, stress analysis, experimental mechanics for stress analysis, and composite materials.

Hyun-Seok Lim received his B.S. degree in Architectural Engineering from Kyeonggi University in 2010 and M.S. degree in Mechanical Engineering from Yeungnam University in Korea in 2012. Mr. Lim is currently is a Ph.D. Candidate under Prof. Hawong in the School of Mechanical Engineering, Yeungnam University, Korea. His research interests include experimental stress analysis and bioengineering.

Dong-Chul Shin received his B.S., M.S., and Ph.D. degrees in Mechanical Engineering from Yeungnam University in 1995, 1997, and 2001, respectively. He studied at the University of Tokyo, Japan as a Post-Doctoral Fellow from 2005 to 2007, He is currently a Professor in the Department of Mechanical Engineering at Koje College, Korea. His research interests include static and dynamic fracture mechanics, stress analysis, and fracture criteria of piezoelectric ceramics.